

Isotope Effects for Lattice Strain and Pseudo Jahn-Teller Distortion of Chiral Cyanide-Bridged Cu(II)-Co(III), Cr(III), and Fe(III) Bimetallic Assemblies

Takashi Akitsu* and Satoru Sonoki

Department of Chemistry, Faculty of Science, Tokyo University of Science, 1-3 Kagurazaka, Shinjuku-ku, Tokyo 162-8601, Japan

Abstract: By substituting H/D and ^{18}O isotopes of water molecules, we prepared co-crystals of one-dimensional cyanide-bridged Cu(II)-Cr(III), Cu(II)-Co(III), and Cu(II)-Fe(III) bimetallic assemblies and mononuclear Cu(II) complexes, $[\text{CuL}_2]_3[\text{M}(\text{CN})_6]_2 \cdot 4\text{H}_2\text{O}$ (L = *trans*-cyclohexane-(1*R*, 2*R*)-diamine; M = Cr, Co, and Fe). Solid state CD and diffuse reflectance electronic spectra exhibited typical difference of metal ions and little isotope effects. While H/D isotope effects emerged as differences of small intermolecular magnetic interactions and obvious shifts of IR bands. Though all compounds exhibited positive thermal expansion of lattice, crystal structures exhibited slight differences associated with Jahn-Teller distortion around Cu(II) coordination environment.

Keywords: Lattice distortion, Jahn-Teller effect, copper, cyanide, isotope.

INTRODUCTION

Recently, we have reported thermally-accessible lattice strain and local pseudo Jahn-Teller distortion of $[\text{CuL}_2]_3[\text{M}(\text{CN})_6]_2 \cdot 4\text{H}_2\text{O}$ (L = *trans*-cyclohexane-(1*R*, 2*R*)-diamine; M = Cr, Co, and Fe) [1]. In its crystal packing of co-crystals of one-dimensional cyanide-bridged Cu(II)-Cr(III), Cu(II)-Co(III) [1], and Cu(II)-Fe(III) [2] bimetallic assemblies and mononuclear Cu(II) complexes, (pseudo) Jahn-Teller effect plays an important role in flexible distortion of crystal structures especially Cu(II) coordination environment. Theoretically, it may be expected that whether magnetic orbital of Cu(II) ion is $d_{x^2-y^2}$ or d_{z^2} , it depends on ligand field strength and bond lengths of axial ligands [3, 4]. Additionally, configuration interaction between $3d_{z^2}$ and $4s$ orbitals mixing is also subjected to tetrahedral as well as tetragonal distortion of Cu(II) coordination environment [5]. However, temperature dependence of pseudo Jahn-Teller distortion of Cu(II) moieties has not been investigated in multi-dimensional cyanide-bridged crystal lattices except for these examples [6, 7]. The results suggested that structural changes associated with pseudo Jahn-Teller distortion of mononuclear *trans*- $[\text{CuL}_2(\text{H}_2\text{O})_2]^{2+}$ moiety induced by external conditions was larger than that of Cu(II) moieties in cyanide-bridged crystal lattices, $\{[\text{CuL}_2]_2[\text{M}(\text{CN})_6]_2\}^{2-} \cdot 2\text{H}_2\text{O}$, whose hydrogen bonds might dominate lattice strain [8-12].

Herein, we investigate isotope effects for $[\text{CuL}_2]_3[\text{M}(\text{CN})_6]_2 \cdot 4\text{H}_2\text{O}$ (L = *trans*-cyclohexane-(1*R*, 2*R*)-diamine; M = Cr, Co, and Fe) about water molecules by substituting H/D and ^{18}O isotopes (**H**, **D**, and **O**) (abbreviated as **Cu-CrH**,

Cu-CrD, **Cu-CrO**, **Cu-CoH**, **Cu-CoD**, **Cu-CoO**, **Cu-FeH**, **Cu-FeD**, and **Cu-FeO**), which may be an important factor for the mononuclear *trans*- $[\text{CuL}_2(\text{H}_2\text{O})_2]^{2+}$ moiety. Solid state CD, diffuse reflectance electronic, and IR spectra, magnetic measurements, and powder and single crystal structure analyses were carried out.

MATERIALS AND METHODOLOGY

General Procedure

Chemicals and solvents of the highest commercial grade available (Kanto Chemical, Tokyo Chemical Industry, and Wako) were used as received without further purification.

Preparations

$[\text{CuL}_2]_3[\text{M}(\text{CN})_6]_2 \cdot 4\text{H}_2\text{O}$, **Cu-CrH**, **Cu-CrD**, **Cu-CrO**, **Cu-CoH**, **Cu-CoD**, **Cu-CoO**, **Cu-FeH**, **Cu-FeD**, **Cu-FeO**, were prepared in similar way to the analogous compounds [1, 2] by employing the corresponding metal sources and water containing isotope atoms.

Preparations of Cu-CrH

Yield 88.1 %. Anal. Calcd. for $\text{C}_{48}\text{H}_{92}\text{Cr}_2\text{Cu}_3\text{N}_{24}\text{O}_4$: C, 42.27; H, 6.80; N, 24.64. Found: C, 42.34; H, 6.79; N, 24.62. IR (cm^{-1} , KBr): 2127 (C \equiv N). XRD ($2\theta/\text{degree}$, $\lambda = 1.54184 \text{ \AA}$) 16.94 and 16.67 for (1 -2 1), 5.77 and 5.80 for (0 0 1), 7.37 and 7.31 for (0 1 0), 8.00 and 7.92 for (0 -1 1), and 11.11 and 11.14 for (1 0 -1) at 100 and 300K, respectively.

Preparations of Cu-CrD

Yield 93.0 %. Anal. Calcd. for $\text{C}_{48}\text{H}_{84}^{2}\text{H}_4\text{Cr}_2\text{Cu}_3\text{N}_{24}\text{O}_4$: C, 42.03; H, 6.76; N, 24.51. Found: C, 42.37; H, 6.71; N, 24.38. IR (cm^{-1} , KBr): 2127 (C \equiv N). XRD ($2\theta/\text{degree}$, $\lambda = 1.54184 \text{ \AA}$) 17.05 and 16.82 for (1 -2 1), 5.83 and 5.77 for (0 0 1), 7.40 and 7.34 for (0 1 0), 8.06 and 7.95 for (0 -1 1), and 11.19 and 11.17 for (1 0 -1) at 100 and 300K, respectively.

*Address correspondence to this author at the Department of Chemistry, Faculty of Science, Tokyo University of Science, 1-3 Kagurazaka, Shinjuku-ku, Tokyo 162-8601, Japan; Tel: +81-3-5228-8271; Fax: +81-3-5261-4631; E-mail: akitsu@rs.kagu.tus.ac.jp

Preparations of Cu-CrO

Yield 88.8 %. Anal. Calcd. for $C_{48}H_{92}Cr_2Cu_3N_{24}^{18}O_4$: C, 42.02; H, 6.76; N, 24.50. Found: C, 42.06; H, 6.59; N, 24.50. IR (cm^{-1} , KBr): 2127 ($C\equiv N$). XRD ($2\theta/degree$, $\lambda = 1.54184 \text{ \AA}$) 17.02 and 16.79 for (1 -2 1), 5.80 and 5.74 for (0 0 1), 7.40 and 7.31 for (0 1 0), 8.03 and 7.92 for (0 -1 1), and 11.22 and 11.14 for (1 0 -1) at 100 and 300K, respectively.

Preparations of Cu-CoH

Yield 76.3 %. Anal. Calcd. for $C_{48}H_{92}Co_2Cu_3N_{24}O_4$: C, 41.84; H, 6.73; N, 24.40. Found: C, 41.57; H, 6.58; N, 24.13. IR (cm^{-1} , KBr): 2114 ($C\equiv N$). XRD ($2\theta/degree$, $\lambda = 1.54184 \text{ \AA}$) 11.43 and 11.34 for (1 0 -1), 11.80 and 11.69 for (0 0 2), 12.30 and 12.15 for (1 -1 0), 19.46 and 19.29 for (1 -2 2), and 21.58 and 21.43 for (1 -1 3) at 100 and 300K, respectively.

Preparations of Cu-CoD

Yield 78.3 %. Anal. Calcd. for $C_{48}H_{84}^2H_4Co_2Cu_3N_{24}O_4$: C, 42.03; H, 6.76; N, 24.51. Found: C, 40.78; H, 6.74; N, 24.69. IR (cm^{-1} , KBr): 2114 ($C\equiv N$). XRD ($2\theta/degree$, $\lambda = 1.54184 \text{ \AA}$) 11.37 and 11.31 for (1 0 -1), 11.75 and 11.69 for (0 0 2), 12.24 and 12.12 for (1 -1 0), 19.46 and 19.37 for (1 -2 2), and 21.55 and 21.49 for (1 -1 3) at 100 and 300K, respectively.

Preparations of Cu-CoO

Yield 74.4 %. Anal. Calcd. for $C_{48}H_{92}Co_2Cu_3N_{24}^{18}O_4$: C, 41.60; H, 6.69; N, 24.26. Found: C, 41.67; H, 6.70; N, 24.21. IR (cm^{-1} , KBr): 2114 ($C\equiv N$). XRD ($2\theta/degree$, $\lambda = 1.54184 \text{ \AA}$) 11.37 and 11.31 for (1 0 -1), 11.72 and 11.69 for (0 0 2), 12.27 and 12.12 for (1 -1 0), 19.49 and 19.37 for (1 -2 2), and 21.55 and 21.37 for (1 -1 3) at 100 and 300K, respectively.

Preparations of Cu-FeH

Yield 73.8 %. Anal. Calcd. for $C_{48}H_{92}Cu_3Fe_2N_{24}O_4$: C, 42.03; H, 6.76; N, 24.51. Found: C, 41.90; H, 6.87; N, 24.28. IR (cm^{-1} , KBr): 2102 ($C\equiv N$). XRD ($2\theta/degree$, $\lambda = 1.54184 \text{ \AA}$) 5.86 and 5.83 for (0 1 0), 7.40 and 7.37 for (1 0 0), 8.03 and 7.95 for (0 0 1), 11.31 and 11.28 for (1 -1 0), and 19.43 and 19.37 for (2 1 1) at 100 and 300K, respectively.

Preparations of Cu-FeD

Yield 91.9 %. Anal. Calcd. for $C_{48}H_{84}^2H_4Cu_3Fe_2N_{24}O_4$: C, 42.03; H, 6.76; N, 24.51. Found: C, 42.37; H, 6.71; N, 24.38. IR (cm^{-1} , KBr): 2102 ($C\equiv N$). XRD ($2\theta/degree$, $\lambda = 1.54184 \text{ \AA}$) 5.86 and 5.86 for (0 1 0), 7.40 and 7.37 for (1 0 0), 8.03 and 7.98 for (0 0 1), 11.34 and 11.28 for (1 -1 0), and 19.43 and 19.27 for (2 1 1) at 100 and 300K, respectively.

Preparations of Cu-FeO

Yield 89.9 %. Anal. Calcd. for $C_{48}H_{92}Cu_3Fe_2N_{24}^{18}O_4$: C, 41.78; H, 6.72; N, 24.36. Found: C, 41.87; H, 6.78; N, 24.40. IR (cm^{-1} , KBr): 2102 ($C\equiv N$). XRD ($2\theta/degree$, $\lambda = 1.54184 \text{ \AA}$) 5.89 and 5.83 for (0 1 0), 7.40 and 7.31 for (1 0 0), 8.03 and 7.92 for (0 0 1), 11.31 and 11.14 for (1 -1 0), and 19.43 and 19.43 for (2 1 1) at 100 and 300K, respectively.

Physical Measurements

Elemental analyses (C, H, N) were carried out on a Perkin Elmer 2400II CHNS/O analyzer at Tokyo University of Science. Infrared spectra were recorded on a JASCO FT-IR 460 plus spectrophotometer in the range of 4000-400 cm^{-1} at 298 K. Electronic spectra were measured on a JASCO V-570 UV/VIS/NIR spectrophotometer in the range of 800–200 nm at 298 K. Circular dichroism (CD) spectra were measured on a JASCO J820 spectropolarimeter in the range of 800-200 nm at 298 K. Powder XRD patterns were also measured by using synchrotron radiation beamline at KEK-PF BL-8B with 8 keV ($\lambda = 1.54184 \text{ \AA}$) under variable temperature apparatus of nitrogen stream equipped with a RIGAKU imaging plate. All the samples were measured for 3 min and constant ring current (440 mA). The magnetic properties were investigated with a Quantum Design MPMS-XL and 5S superconducting quantum interference device magnetometer (SQUID) at an applied field 0.5 T in a temperature range 5-300 K. Powder samples were measured in a pharmaceutical cellulose capsule. The apparatus signals and the diamagnetic corrections were evaluated from Pascal's constants.

X-ray Crystallography

Blue violet prismatic single crystals of **Cu-CoH** (0.26 x 0.20 x 0.18 mm), **Cu-CoD** (0.26 x 0.24 x 0.19 mm), and **Cu-CoO** (0.20 x 0.18 x 0.16 mm) were glued on top of a glass fiber and coated with a thin layer of epoxy resin to measure the diffraction data. The X-ray intensities were measured at 130 K for **Cu-CoH** and **Cu-CoO** and 100, 130 and 296 K for **Cu-CoD** with graphite-monochromated Mo $K\alpha$ radiation ($\lambda = 0.71073 \text{ \AA}$) on a Bruker APEX2 CCD diffractometer. The structures were solved by direct methods using SHELXS97 [13] and expanded by Fourier techniques in a SAINT program package [14] (including SHELXTL version). The structures were refined on F^2 anisotropically for non-hydrogen atoms by full-matrix least-square methods with SHELXL97 [13]. Empirical absorption corrections were applied by a program SADABS [15]. All the non-hydrogen atoms were refined anisotropically. The hydrogen atoms were included in geometrically calculated position and refined by using riding model. Since hydrogen atoms could not be observed in the different Fourier map, we could not introduce hydrogen atoms of water molecules connected to O1 through O5 atoms. Although residual electron density was also found in the difference Fourier maps, the models containing these peaks as water molecules resulted in increase of R-values. Therefore, we could not assign them and we could not discuss hydrogen bonds closely. These bad results in refinement are mainly due to thermal vibration of oxygen atoms of crystalline water.

Crystallographic data for **Cu-CoH**. [$T = 130(2) \text{ K}$] $C_{48}H_{84}Co_2Cu_3N_{24}O_5$, triclinic, PI , $a = 8.3377(11) \text{ \AA}$, $b = 12.6477(16) \text{ \AA}$, $c = 16.019(2) \text{ \AA}$, $\alpha = 105.575(2)^\circ$, $\beta = 99.018(2)^\circ$, $\gamma = 95.841(2)^\circ$, and $V = 1588.6(4) \text{ \AA}^3$, and $Z = 1$, $D_c = 1.449 \text{ Mg m}^{-3}$, $R_1 = 0.0369$, $wR_2 = 0.1343$ (7894 reflections), $S = 0.787$, $\mu = 1.561 \text{ mm}^{-1}$. Flack value is equal to -0.006(18).

Crystallographic data for **Cu-CoD**. [$T = 130(2) \text{ K}$] $C_{48}H_{84}Co_2Cu_3N_{24}O_5$, triclinic, PI , $a = 8.3228(11) \text{ \AA}$, $b =$

12.6426(17) Å, $c = 16.007(2)$ Å, $\alpha = 105.579(2)^\circ$, $\beta = 99.058(2)^\circ$, $\gamma = 95.799(2)^\circ$, and $V = 1583.9(4)$ Å³, and $Z = 1$, $D_c = 1.453$ Mgm⁻³, $R_1 = 0.0317$, $wR_2 = 0.0907$ (9786 reflections), $S = 0.825$, $\mu = 1.566$ mm⁻¹. Flack value is equal to 0.019(11).

Crystallographic data for **Cu-CoD**. [$T = 100(2)$ K] $C_{48}H_{88}Co_2Cu_3N_{24}O_5$, triclinic, PI , $a = 8.3374(3)$ Å, $b = 12.6329(5)$ Å, $c = 16.0129(6)$ Å, $\alpha = 105.45(2)^\circ$, $\beta = 99.11(2)^\circ$, $\gamma = 95.7310(10)^\circ$, and $V = 1587.13(10)$ Å³, and $Z = 1$, $D_c = 1.454$ Mgm⁻³, $R_1 = 0.0241$, $wR_2 = 0.0667$ (9322 reflections), $S = 0.955$, $\mu = 1.563$ mm⁻¹. Flack value is equal to -0.012(8).

Crystallographic data for **Cu-CoD**. [$T = 296(2)$ K] $C_{48}H_{86}Co_2Cu_3N_{24}O_5$, triclinic, PI , $a = 8.3941(4)$ Å, $b = 12.7209(7)$ Å, $c = 16.1119(9)$ Å, $\alpha = 105.7130(10)^\circ$, $\beta = 98.6270(10)^\circ$, $\gamma = 96.2530(10)^\circ$, and $V = 1617.07(15)$ Å³, and $Z = 1$, $D_c = 1.425$ Mgm⁻³, $R_1 = 0.0288$, $wR_2 = 0.0760$ (9518

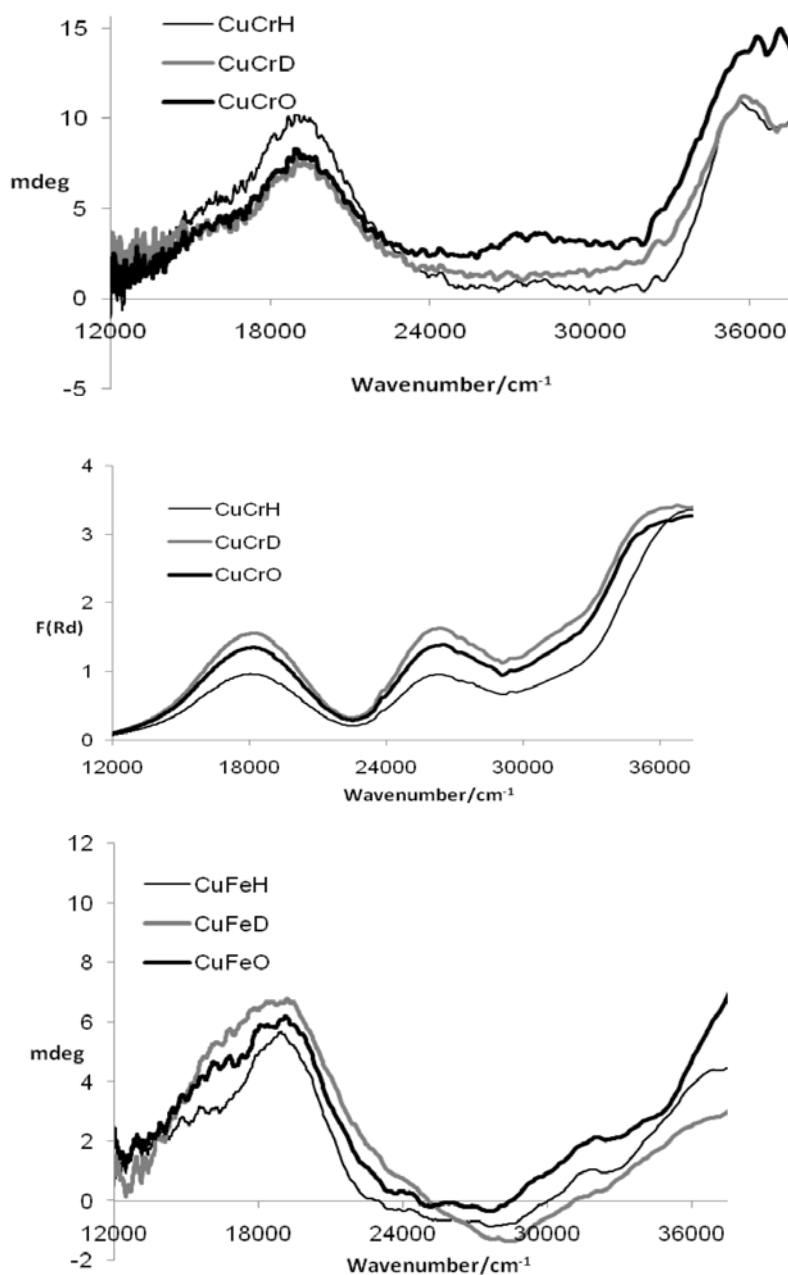
reflections), $S = 1.027$, $\mu = 1.534$ mm⁻¹. Flack value is equal to -0.003(9).

Crystallographic data for **Cu-CoO**. [$T = 130(2)$ K] $C_{48}H_{84}Co_2Cu_3N_{24}O_5$, triclinic, PI , $a = 8.317(4)$ Å, $b = 12.651(6)$ Å, $c = 16.025(2)$ Å, $\alpha = 105.662(7)^\circ$, $\beta = 99.080(7)^\circ$, $\gamma = 95.627(7)^\circ$, and $V = 1585.3(14)$ Å³, and $Z = 1$, $D_c = 1.452$ Mgm⁻³, $R_1 = 0.0454$, $wR_2 = 0.1534$ (5688 reflections), $S = 1.012$, $\mu = 1.564$ mm⁻¹. Flack value is equal to 0.00(3).

RESULTS AND DISCUSSION

CD and Diffuse Reflectance Electronic Spectra

Fig. (1) shows solid state CD (as KBr pellets) and diffuse reflectance electronic spectra for **Cu-Cr**, **Cu-Fe**, and **Cu-Co** (**H**, **D**, and **O**) complexes. For Cr(III), Fe(III), and Co(III) complexes, little differences by isotope effects could be observed, while drastic differences of CT (charge transfer) bands could be observed by substituting metal ions, namely



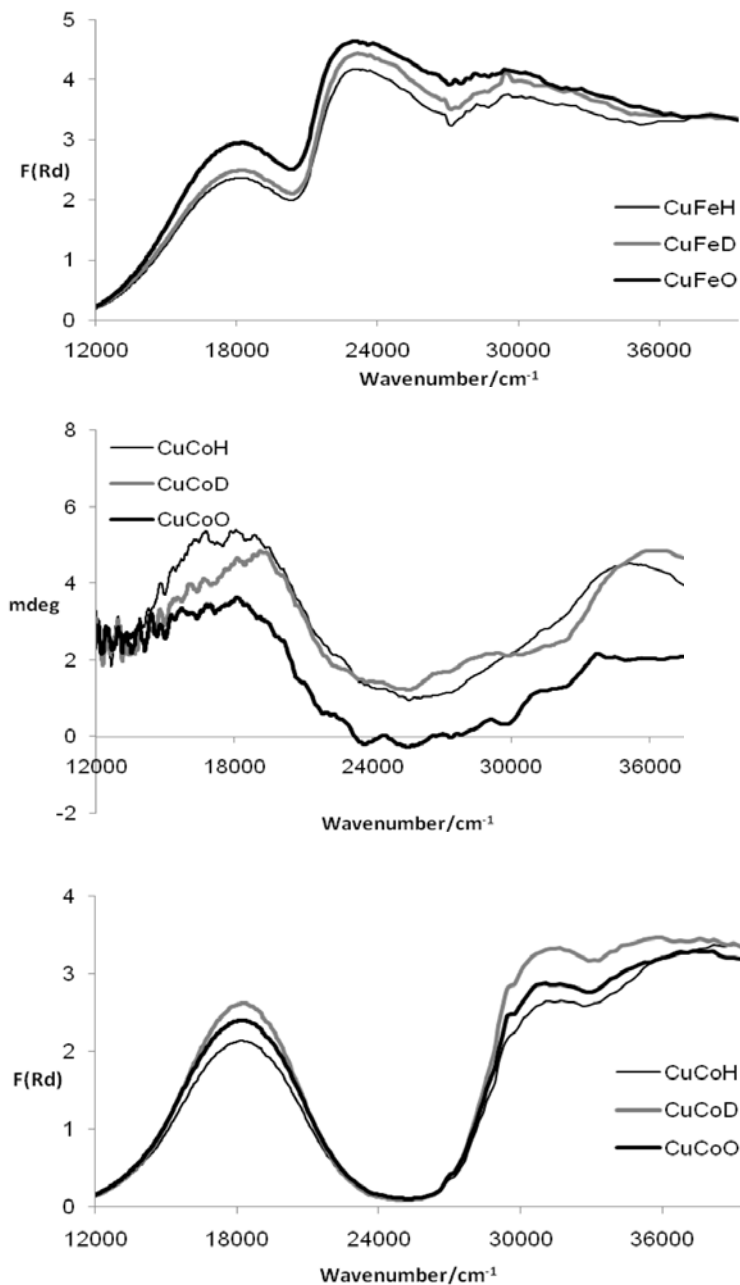


Fig. (1). [above] Solid State CD (as KBr pellets) and [below] diffuse reflectance electronic spectra for [left] **Cu-Cr** (**H** [blue], **D** [red], and **O** [green]), [middle] **Cu-Fe** (**H**, **D**, and **O**), and [right] **Cu-Co** (**H**, **D**, and **O**) complexes at 300 K.

$[\text{Cr}(\text{CN})_6]^{3-}$, $[\text{Fe}(\text{CN})_6]^{3-}$, and $[\text{Co}(\text{CN})_6]^{3-}$. Previously, we also reported that CD spectra as follows [1]: a positive peak at 19300 cm^{-1} and negative peaks at 16600 cm^{-1} and 34000 cm^{-1} for **Cu-CrH**, a positive peak at 19100 cm^{-1} , 27000 cm^{-1} (shoulder), and a negative peak at 31600 cm^{-1} for **Cu-CoH**, and positive d-d peak at 14500 cm^{-1} , positive CT peak at 18900 cm^{-1} , and negative CT peak at 28600 cm^{-1} for **Cu-FeH** [2]. The corresponding diffuse reflectance electronic spectra were reported as follows [1, 2, 16]: d-d bands appeared at 19100 , 19800 , and 19400 cm^{-1} , $\pi-\pi^*$ bands appeared at 28900 , 26000 , and 26500 cm^{-1} for **Cu-CrH**, **Cu-CoH**, and **Cu-FeH**, respectively, and CT bands appeared at 600 and 22900 cm^{-1} for **Cu-CoH** and **Cu-FeH**, respectively.

Magnetic Properties

Fig. (2) shows temperature dependence of the $\chi_M T$ values per $[\text{CuL}_2]_3[\text{M}(\text{CN})_6]_2 \cdot 4\text{H}_2\text{O}$ units of a powder sample of **Cu-Cr**, **Cu-Co**, and **Cu-Fe** (**H**, **D**, and **O**) complexes at 0.5 T. All three compounds are composed of paramagnetic one-dimensional $\text{Cu}^{\text{II}}\text{M}^{\text{III}}_2$ chains and paramagnetic mononuclear Cu^{II} moiety, though superexchange interactions through cyanide-bridged are mainly dependent on $[\text{Cr}(\text{CN})_6]^{3-}$, $[\text{Fe}(\text{CN})_6]^{3-}$, and $[\text{Co}(\text{CN})_6]^{3-}$ moieties regardless of isotopes effects. For example, we have reported for **Cu-CoH** in the previous paper [1] as follows: The $\chi_M T$ value is $0.694\text{ cm}^3\text{Kmol}^{-1}$ at 300 K, which is smaller than the expected value ($1.625\text{ cm}^3\text{Kmol}^{-1}$) for uncoupled $\text{Cu}^{\text{II}}_3\text{Co}^{\text{III}}_2$ system of

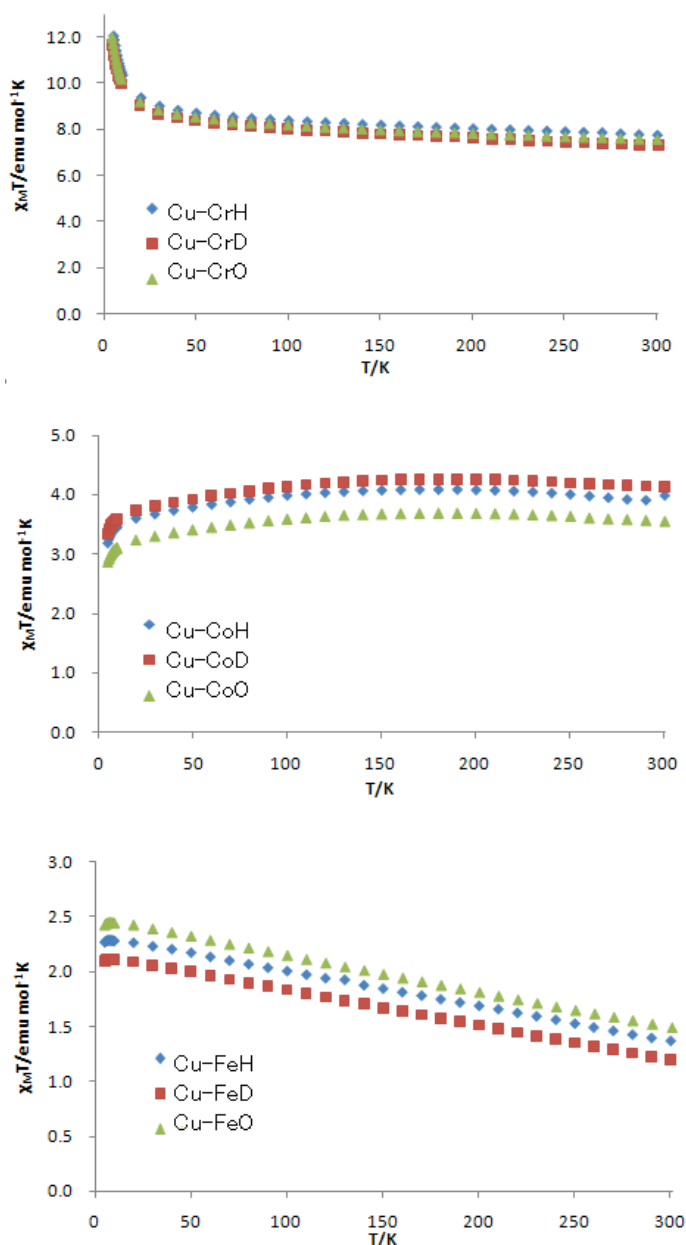


Fig. (2). Temperature dependence of χ_{MT} values for [above] **Cu-Cr** (**H** [diamond], **D** [square], and **O** [triangle]), [middle] **Cu-Fe** (**H**, **D**, and **O**), and [below] **Cu-Co** (**H**, **D**, and **O**) at 0.5 T.

Co^{III} ($S = 0$) and Cu^{II} ($S = 1/2$). On cooling, the χ_{MT} value gradually increases up to $1.10 \text{ cm}^3 \text{Kmol}^{-1}$ at 5 K. However, slight isotope effects (**H**, **D**, and **O**) within the same compounds must be ascribed to intermolecular hydrogen bonds.

IR spectra

Fig. (3) shows IR spectra of **Cu-Cr**, **Cu-Co**, and **Cu-Fe** (**H**, **D**, and **O**) complexes. The features of cyanide stretching bands depend on the types (bridged or terminal) of cyanide ligands and weight of metal ions (namely $[\text{Cr}(\text{CN})_6]^{3-}$, $[\text{Fe}(\text{CN})_6]^{3-}$, and $[\text{Co}(\text{CN})_6]^{3-}$ moieties), and appear at 2127, 2114, and 2102 cm^{-1} , respectively. However, little isotope effects could be observed as cyanide stretching bands for all three compounds (see preparations). The splitting of cyanide bands is attributed to the types of cyanide ligands, which is not clear (not shown) [1]. Although O-H bands can vary by

both D and ^{18}O substitution, characteristic band shift around 830 , 880 , 1200 cm^{-1} could be observed only for **Cu-CrD**, **Cu-CoD**, and **Cu-FeD** obviously. The H/D isotope effects emerged as differences of small intermolecular magnetic interactions and clear shift of IR bands.

Crystal Structures

Fig. (4) shows important parts of crystal packing of **Cu-CoD**, which is isostructural to previously reported **Cu-Co**, **Cu-Cr**, and **Cu-Fe** essentially. Tables 1 and 2 summarize selected (axial elongated bonds due to Jahn-Teller distortion of three Cu(II) atoms) isotope differences of **Cu-Co** (**H**, **D**, and **O**) complexes at 130 K and temperature dependence of **Cu-CoD** at 100, 130, and 296 K respectively. As mentioned for the IR spectra of isotope effects caused by H/D or $^{16}\text{O}/^{18}\text{O}$ substitution, structural differences caused by hydro-

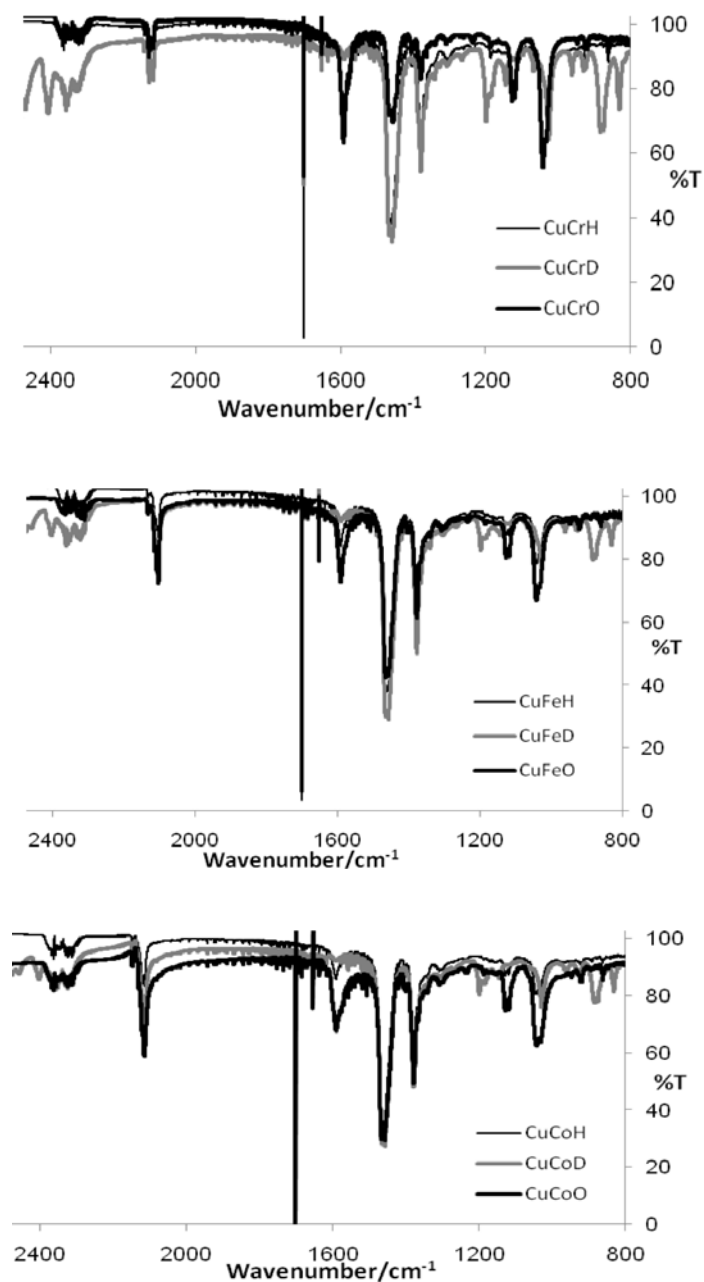


Fig. (3). IR spectra for for [above] **Cu-Cr** (**H** [plain], **D** [gray], and **O** [bold]), [middle] **Cu-Fe** (**H**, **D**, and **O**), and [below] **Cu-Co** (**H**, **D**, and **O**) at 300 K.

gen bonds or atomic weight of water molecules may be expected for crystal structures. However, structural evidence of isotopes of water molecules could not be detected as Jahn-Teller distorted Cu(II) coordination environment not other positions of non-hydrogen atoms for **Cu-Co** (**H**, **D**, and **O**) complexes. Previously, we reported that thermally crystal changes associated with pseudo Jahn-Teller effect for **Cu-Co** and **Cu-Cr** could be significantly found in axial bond distances of the mononuclear *trans*-[CuL₂(H₂O)₂]²⁺ moiety, while not found in Cu(II) moieties involved cyanide-bridged crystal lattices, {[CuL₂]₂[M(CN)₆]₂}²⁻·2H₂O [1]. As stated in the preparations section, powder XRD by means of synchrotron radiation exhibited positive thermal expansion of crystal lattice for all compounds of **Cu-Co**, **Cu-Cr**, and **Cu-Fe** (**H**, **D**, and **O**) complexes at 100 and 300 K normally. They

exhibit positive thermal expansion as a function of temperature continuously without structural phase transition, and do not exhibit negative thermal expansion of cyanide complexes [17-20] accompanying with losing crystalline water molecules. In general, O-D hydrogen bonds are weaker than O-H ones. Although little structural differences between **Cu-CrH** and **Cu-CrD** could be observed at constant temperature of 130 K, temperature dependences of local geometries for **Cu-CrD** are investigated at 100 and 298 K. However, Table 2 indicated normal structural changes even for **Cu-CoD**. In this way, differences detected by IR spectra and magnetic properties among **H**, **D**, and **O** complexes are too slight to detect crystallographically [21] in the range of our study by present procedures.

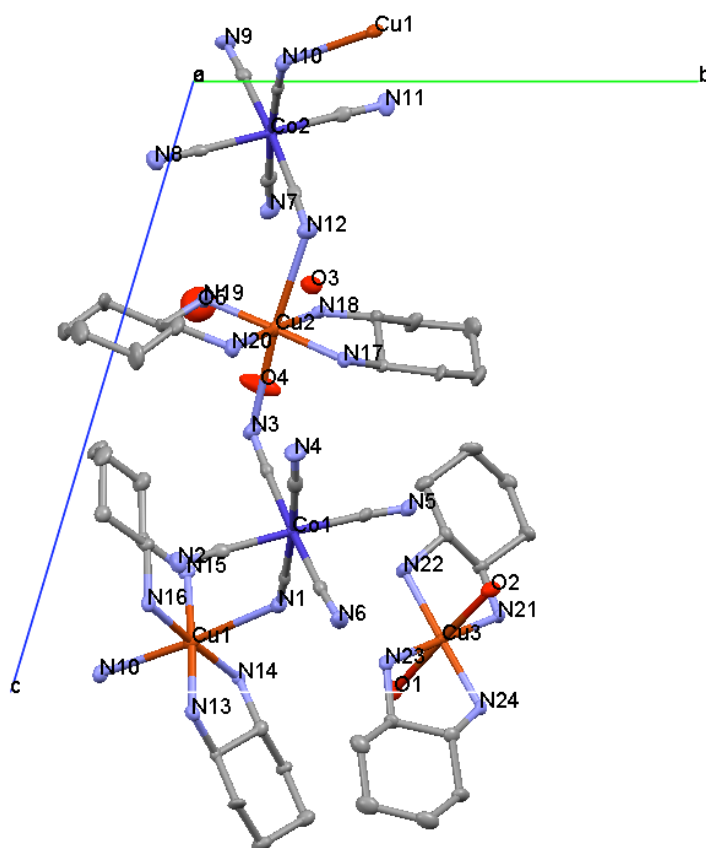


Fig. (4). Crystal packing for Cu-CoD with selected atomic labeling schemes.

Table 1. Selected Bond Distances (Å) of Cu-CoH, Cu-CoD, and Cu-CoO at 130 K

	Cu-CoH	Cu-CoD	Cu-CoO
Cu1 - N3	2.7647(7)	2.7639(4)	2.7512(13)
Cu1 - N12	2.6493(7)	2.6286(4)	2.6172(14)
Cu2 - N1	2.6487(7)	2.6373(4)	2.6525(13)
Cu2 - N7	2.6552(7)	2.6524(4)	2.6576(12)
Cu3 - O1	2.4560(6)	2.4470(4)	2.4522(11)
Cu3 - O2	2.4631(6)	2.4644(3)	2.4665(11)

Table 2. Temperature Dependence of Selected Bond Distances (Å) of Cu-CoD at 100, 130, and 296 K

	100 K	130 K	296 K
Cu1 - N3	2.753(3)	2.7639(4)	2.811(4)
Cu1 - N12	2.647(3)	2.6286(4)	2.651(4)
Cu2 - N1	2.628(3)	2.6373(4)	2.669(4)
Cu2 - N7	2.646(3)	2.6524(4)	2.708(4)
Cu3 - O1	2.431(3)	2.4470(4)	2.478(4)
Cu3 - O2	2.454(3)	2.4644(3)	2.496(4)

CONCLUSION

By substituting H/D and ^{18}O isotopes of water molecules, we prepared bimetallic assemblies, Cu-CrH, Cu-CrD, Cu-

CrO, Cu-CoH, Cu-CoD, Cu-CoO, Cu-FeH, Cu-FeD, and Cu-FeO. Solid state CD and diffuse reflectance electronic spectra exhibited typical difference of d-d and CT bands due

to Cr(III), Co(III), and Fe(III) metal ions without obvious differences due to isotope effect. Tuning of strength of intermolecular hydrogen bonds by substituting H/D better than $^{16}\text{O}/^{18}\text{O}$ resulted in small differences of magnetic properties and significant shift of IR bands associated with O-D bands. However, structural evidence of isotopes of water molecules could not be detected as Jahn-Teller distorted Cu(II) coordination environment nor displacement of non-hydrogen atoms. Additionally, powder XRD by means of synchrotron radiation exhibited normally positive thermal expansion of crystal lattice for all compounds.

SUPPLEMENTARY DATA

CCDC (782124-782418) contains the supplementary crystallographic data. These data can be obtained free of charge via <http://www.ccdc.cam.ac.uk/conts/retrieving.html>, or from the Cambridge Crystallographic Data Centre, 12 Union Road, Cambridge CB2 1EZ, UK; fax: (+44) 1223-336-033; or e-mail: deposit@ccdc.cam.ac.uk.

ACKNOWLEDGEMENTS

We are gratefully acknowledged to the Materials Design and Characterization Laboratory, Institute for Solid State Physics, the University of Tokyo for the use of the SQUID facilities and KEK-PF BL-8B (2008G526) for X-ray crystallography using synchrotron radiation.

REFERENCES

- [1] Akitsu T, Einaga Y, Yoza K. Thermally-accessible lattice strain and local pseudo jahn-teller distortion in various dimensional $\text{Cu}^{\text{II}}\text{-M}^{\text{III}}$ bimetallic cyanide-bridged assemblies. *Open Inorg Chem J* 2008; 2: 1-10.
- [2] Coronado E, Gimenez-Saiz C, Martinez-Agudo JM, Muez A, Romero FM, Stoeckli-Evans H. Design of chiral magnets: cyanide-bridged bimetallic assemblies based on cyclohexane-1,2-diamine. *Polyhedron* 2003; 22: 2435-40.
- [3] Falvello LR, Jahn-Teller effects in solid-state co-ordination chemistry. *J Chem Soc Dalton Trans* 1997; 4463-75.
- [4] Halcrow MA. Interpreting and controlling the structures of six-coordinate copper(II) centres – When is a compression really a compression? *Dalton Trans* 2003; 4375-84.
- [5] Akitsu T, Einaga Y. Thermal and photo-responsibility of axial semi-coordination bonds in Copper(II) complex. *Bull Chem Soc Jpn* 2004; 77: 763-4.
- [6] Akitsu T, Einaga Y. Structures, magnetic properties, and XPS of one-dimensional cyanide-bridged $\text{Cu}^{\text{II}}\text{-Ni}^{\text{II}}/\text{Pt}^{\text{II}}$ bimetallic assembly complexes. *Inorg Chim Acta* 2007; 360: 497-505.
- [7] Akitsu T, Endo Y. The one-dimensional chain structure of $\text{Cu}(\text{N-Eten})_2\text{Pd}(\text{CN})_4$ (N-Eten = N-ethylethylenediamine). *Acta Cryst E* 2009; 65: m406-m7.
- [8] Sereda O, Stoeckli-Evans H, Dolomanov O, Filinchuk Y, Pattison P. Transformation of a chiral nanoporous bimetallic cyano-bridged framework triggered by dehydration/rehydration. *Crystal Growth Des* 2009; 9: 3168-78.
- [9] Sereda O, Neels A, Stoeckli F, Stoeckli-Evans H, Filinchuk Y. Sponge-like reversible transformation of a bimetallic cyanometalate polymer. *Crystal Growth Des* 2008; 8: 2307-11.
- [10] Sereda O, Neels A, Stoeckli F, Stoeckli-Evans H. Chiral bimetallic assemblies and coordination polymers based on tetracyanonickelate: a striking reversible structural transformation. *Crystal Growth Des* 2008; 8: 3380-4.
- [11] Akitsu T, Einaga Y. Extremely long axial Cu-N bonds in chiral one-dimensional zigzag cyanide-bridged $\text{Cu}^{\text{II}}\text{-Ni}^{\text{II}}$ and $\text{Cu}^{\text{II}}\text{-Pt}^{\text{II}}$ bimetallic assemblies. *Inorg Chem* 2006; 45: 9826-33.
- [12] Akitsu T, Einaga Y. Tuning of electronic properties of one-dimensional cyano-bridged $\text{Cu}^{\text{II}}\text{-Ni}^{\text{II}}$, $\text{Cu}^{\text{II}}\text{-Pd}^{\text{II}}$, and $\text{Cu}^{\text{II}}\text{-Pt}^{\text{II}}$ bimetallic assemblies by stereochemistry of ligands. *Inorg Chim Acta* 2008; 361: 36-42.
- [13] Sheldrick GM. A short history of SHELX. *Acta Crystallogr A* 2008; 64: 112-22.
- [14] Bruker. *SMART and SAINT*. Bruker AXS Inc., Madison, Wisconsin, USA, 1998.
- [15] Sheldrick GM. *SADABS*. Program for empirical absorption, correction of area detector data. University of Gottingen: Germany, 1996.
- [16] Lever ABP. *Inorganic electronic spectroscopy*. 2nd ed. Amsterdam: Elsevier 1984.
- [17] Goodwin AL, Chapman KW, Kepert CJ. Guest-dependent negative thermal expansion in nanoporous prussian blue analogues $\text{M}^{\text{II}}\text{Pt}^{\text{IV}}(\text{CN})_6 \cdot x\{\text{H}_2\text{O}\}$ ($0 < x < 2$; $\text{M} = \text{Zn}, \text{Cd}$). *J Am Chem Soc* 2005; 127: 17980-1.
- [18] Goodwin AL, Kennedy BJ, Kepert CJ. Thermal expansion matching via framework flexibility in zinc dicyanomellates. *J Am Chem Soc* 2009; 131: 6334.
- [19] Goodwin AL, Calleja M, Conterio MJ, *et al.* Colossal positive and negative thermal expansion in the framework material $\text{Ag}_3[\text{Co}(\text{CN})_6]$. *Science* 2008; 319: 794-7.
- [20] Korcok JL, Katz MJ, Leznoff DB. Impact of metallophilicity on “colossal” positive and negative thermal expansion in a series of isostructural dicyanomellate coordination polymers. *J Am Chem Soc* 2009; 131: 4866-71.
- [21] Akitsu T, Sano K. Analogy of van't Hoff relationship for thermally-accessible lattice strain of Copper(II) complex. *Netsu Sokutei* 2009; 36: 244-6.

Received: June 24, 2010

Revised: December 29, 2010

Accepted: January 10, 2011

© Akitsu and Sonoki; Licensee *Bentham Open*.

This is an open access article licensed under the terms of the Creative Commons Attribution Non-Commercial License (<http://creativecommons.org/licenses/by-nc/3.0/>) which permits unrestricted, non-commercial use, distribution and reproduction in any medium, provided the work is properly cited.